

Received March 28, 2019, accepted April 19, 2019, date of publication April 23, 2019, date of current version June 11, 2019.

Digital Object Identifier 10.1109/ACCESS.2019.2912917

# Selective Dynamic Coded Cooperative Communications for Multi-Hop Underwater Acoustic Sensor Networks

YOUGAN CHEN<sup>1,2</sup>, (Member, IEEE), XIAOTING JIN<sup>1,2</sup>, LEI WAN<sup>3</sup>, (Member, IEEE),  
XIAOKANG ZHANG<sup>1,2</sup>, AND XIAOMEI XU<sup>1,2</sup>

<sup>1</sup>Key Laboratory of Underwater Acoustic Communication and Marine Information Technology (Xiamen University), Ministry of Education, Xiamen 361005, China

<sup>2</sup>Shenzhen Research Institute of Xiamen University, Shenzhen 518000, China

<sup>3</sup>College of Underwater Acoustic Engineering, Harbin Engineering University, Harbin 150001, China

Corresponding author: Xiaomei Xu (xmxu@xmu.edu.cn)

This work was supported in part by the Basic Research Program of Science and Technology of Shenzhen, China, under Grant JCYJ20170818141735140, in part by the National Key Research and Development Program of China under Grant 2016YFC1400200, in part by the National Natural Science Foundation of China under Grant 41476026, Grant 41676024, and Grant 61801139, in part by the Fundamental Research Funds for the Central Universities of China under Grant 20720180078 and Grant 20720180105, and in part by the Natural Science Foundation of Fujian Province of China under Grant 2018J05071.

**ABSTRACT** Due to the limitation of acoustic velocity in underwater environments, propagation delay is a horrible problem in multi-hop underwater acoustic sensor networks (UW-ASNs). In this paper, we proposed an improved scheme of dynamic coded cooperation called selective dynamic coded cooperation (S-DCC) for the multi-hop UW-ASNs, aiming at reducing the end-to-end delay and improving the transmission efficiency. In S-DCC scheme, the cooperative node actively transmits blocks with limited redundancy; yet the receiver only selectively receives those cooperative blocks depending on its own decoding conditions. The S-DCC scheme can utilize the retransmission mechanism adequately to eliminate the waiting time and drastically shorten the overall transmission time, the gain of which increases linearly with the number of hops. Concerning the transmission delay and energy consumption, we evaluated the performances with the different maximum number of retransmissions and different data burst sizes for the proposed S-DCC scheme and other compared schemes. The simulation results showed that the proposed S-DCC scheme could achieve decent outage performance and reduce the end-to-end delay effectively without extra energy consumption compared with other existing schemes, especially for the cases with low transmission signal to noise ratio. Sea test data were also adopted to further verify the conclusions.

**INDEX TERMS** Energy consumption, multi-hop networks, end-to-end delay, underwater acoustic communications.

## I. INTRODUCTION

With the development of the exploration of the oceans, the traditional node-to-node underwater acoustic communication has been transformed into networks. Underwater Acoustic Sensor Networks (UW-ASNs) have been extensively used in marine research, commercial and military applications [1], [2]. However, the design of UW-ASNs is a challenging task due to the harsh characteristics of underwater acoustic channels, such as limited frequency,

distance-dependent bandwidth, high propagation delay, high bit error rates and temporary loss of connectivity.

In underwater acoustic environments, much more transmission power is required for direct long distance communication. Hence the long link is usually divided into several short links in multi-hop transmissions where the data can be transmitted at a higher rate in each hop. This is because multi-hop system can decrease signal attenuation and provide more available bandwidth [3], which is especially appealing to underwater acoustic channels. On the other hand, most sensor nodes in multi-hop UW-ASNs are battery powered and are difficult to recharge or replace, which calls for attention to the transmission efficiency during the design of UW-ASNs.

The associate editor coordinating the review of this manuscript and approving it for publication was Cunhua Pan.

Generally, the end-to-end delay and energy efficiency are the key metrics considered in the design of UW-ASNs. There have been several research articles [4]–[6] about the end-to-end delay and energy-efficiency in linear UW-ASNs with different focuses. In [4], it proposes an energy-efficiency grid routing based on 3D cubes for UW-ASNs, considering the 3D changing topology, high propagation delay, node mobility and density. The literature in [5] shows the bandwidth-distance, power-distance and delay-distance relationships, respectively, for energy-efficient design in UW-ASNs. Furthermore, in [6], the tradeoffs between energy consumption and network connectivity in UW-ASNs are investigated. Although the aforementioned papers provide some closed-form approximate models, it is still difficult to draw a conclusion for the relationship between energy consumption and multi-hop network design in the string UW-ASNs. Moreover, most of the references do not consider the cooperative transmission.

To combat underwater channel unreliability and large path losses, cooperative transmission has been applied in underwater acoustic communications as an ideal solution. In [7], it demonstrates the superiority of cooperative underwater acoustic communication systems over the point-to-point systems, and they meet the requirements of UW-ASNs. For the cooperative communications, the design of relay strategy is crucial, and lots of schemes have been studied, such as amplify-and-forward (AF), decode-and-forward (DF) and compression-and-forward (CF) [8], [9]. Especially, dynamic coded cooperation (DCC) [10]–[12] has been proposed by investigating the combination of coding and relay cooperation. In [13], we proposed orthogonal-frequency-division multiplexing (OFDM) modulated DCC for three-node underwater acoustic cooperative networks, where the relay node can randomly access the point-to-point transmission procedure and enhance the communications by exploiting the benefit of rate-compatible coding. As shown in [13], significant gain was achieved by DCC in underwater acoustic channels, and therefore it is a promising technique in the design of future UW-ASNs. However, in adverse channel conditions, the existing DCC protocols require the cooperative node to retransmit the data *with feedback signal* in each hop. Once in the multi-hop scenario of UW-ASNs, this will result in an accumulative effect of end-to-end delay due to the request time for retransmission in each hop. Hence there still exists serious end-to-end delay problems in the DCC protocol [14] when further applied to the multi-hop UW-ASNs. In order to reduce the end-to-end delay and make DCC more suitable for the multi-hop scenario, in this paper we propose an improved scheme based on the DCC protocol, called Selective Dynamic Coded Cooperation (S-DCC) protocol as the relay strategy for multi-hop UW-ASNs.

The main contributions of this paper are as bellow:

1) Presenting an improved scheme named S-DCC based on the DCC protocol. In the proposed protocol, the cooperative nodes retransmit blocks actively and redundantly, and the receiver nodes selectively receive and deal with these blocks

according to its instant decoding results. Hence the waiting time of feedback signal sent by the receiver to the cooperative node can be used for the redundant blocks' transmission, although they might not be adopted for dynamic decoding eventually. In other words, since the request time for retransmission is eliminated, S-DCC can drastically shorten the overall transmission time for the multi-hop UW-ASNs system compared with the existing DCC protocols.

In addition, the main idea of Cooperative Hybrid Automatic Repeat reQuest (C-HARQ) protocol for UW-ASNs in [15] is to retransmit the *erroneous part* instead of entire packet to reduce the delay from the cooperative node, which essentially merges Cooperative ARQ (C-ARQ) with a Hybrid ARQ (HARQ) technique. Yet it does not concern the DCC protocol or S-DCC protocol. Instead of retransmitting the *erroneous part packet*, the cooperative node transmits part of the *partial coded packet* in DCC or S-DCC protocol, where the *partial coded packet* can be arbitrarily added to the received data as a whole codeword for decoding, so as to utilize the benefits of both the broadcasting listening and cooperation phases. More details about the design of C-ARQ, HARQ and C-HARQ in underwater acoustic channels can be found in [15].

2) Investigating the delay-energy relationship in multi-hop UW-ASNs for both S-DCC and DCC protocols. We compare the outage probability, end-to-end delay and energy consumption of the S-DCC, DCC, C-ARQ protocols and the conventional stop and wait ARQ (S&W ARQ) protocol in the multi-hop UW-ASNs. Simulation results show that, the proposed S-DCC scheme can achieve decent outage performance and reduce end-to-end delay effectively without extra energy consumption, compared with other existing schemes. The proposed S-DCC scheme is a feasible cooperative strategy for low transmission Signal to Noise Ratio (SNR). The sea test data are adopted to further verify the conclusions.

3) Given the target performance, e.g., the outage probability of the multi-hop UW-ASNs system  $P^{\text{out}} \leq 10^{-2}$ , we study the performances with different maximum numbers of retransmissions and block sizes of data burst for both S-DCC and DCC protocols, which will help the design and application of the proposed scheme in practice.

The rest of this paper is organized as follows. In Section II, the network topology of multi-hop UW-ASNs, underwater acoustic channels and energy consumption for underwater acoustic transmission are introduced. Section III presents the proposed S-DCC protocol in detail, including its end-to-end delay and energy consumption for multi-hop UW-ASNs system. Simulation and experimental results are presented in Section IV and V, respectively. Finally, Section VI concludes this paper.

## II. SYSTEM MODEL

In this section, we present the network topology and underwater energy consumption model. Table 1 summarizes key symbols used throughout the paper.

TABLE 1. List of key symbols.

Symbol	Description
S	Source node
D	Destination node
$R_i$	Relay node $i$ ( $i=1,2,\dots,N_h-1$ )
$C_i$	Cooperative node $i$ ( $i=1,2,\dots,N_h$ )
$N_h$	Number of hops
$d$	Source to destination distance
$k$	Spreading factor
$f$	Frequency
$\alpha(f)$	Absorption coefficient
$c$	Propagation velocity of sound wave in sea water
$P_t$	Power consumption for transmitting
$P_r$	Power consumption for receiving
$P_{idle}$	Power consumption for idle mode operating
$E_{hop,i}$	Energy consumed in the $i$ -th hop
$E_{tx}^{block}$	Energy consumed in transmitting one block
$E_{rx}^{block}$	Energy consumed in receiving one block
$E_{idle}$	Energy consumed in the idle mode
$E_{tx}^{ACK/NAK}$	Energy consumption in transmitting ACK or NAK
$E_{rx}^{ACK/NAK}$	Energy consumption in receiving ACK or NAK
$T_{hop,i}$	End-to-end delay in the $i$ -th hop
$T_{block}$	Block transmission time
$T_{idle}$	Idle mode operating time
$M_{max}$	Maximum transmission times of cooperative node
$N_{ii}$	Data size in cooperative node received for decoding
$N_{coop}$	Date size in cooperative node transmitted for cooperation
$N_{bt}$	Data burst size
$I_{bt}$	Information block size
$K$	OFDM subcarrier number
$P^{out}$	Outage probability
$MI$	Mutual information
$r$	Information rate
$P/\sigma_w^2$	Transmission signal to noise ratio

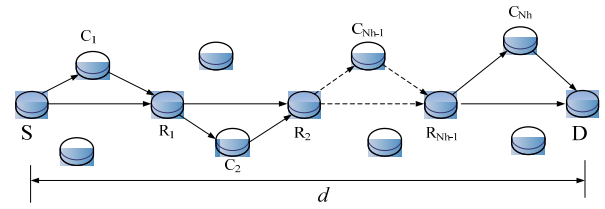


FIGURE 1. A  $N_h$ -hop cooperative network adopting the coded cooperation scheme.

the transmission of the cooperative node  $C_i$  can only be heard by the neighboring relay nodes  $R_{i-1}$  and  $R_i$ . With this assumption, the data transmission in one hop will not affect the next hop;

3) The transmission path is predetermined by the optimal routing algorithm for a given S-D pair, and in each hop, the best node can be selected as the cooperative node in the candidate nodes. The designs of optimal routing algorithm, including the selection of relay nodes  $R_i$  ( $i = 1, 2, \dots, N_h - 1$ ) and cooperative nodes  $C_i$  ( $i = 1, 2, \dots, N_h - 1$ ), are beyond the scope of this paper.

According to the above assumptions, since each hop consisting of source-relay-destination 3 nodes is predetermined in the multi-hop network, and the transmission in each hop will not be received by the next hop, the data transmission is indeed carried out strictly hop by hop. In this case, there is no impact between the transmission inside different hops, and the performance analysis of the energy consumption, delay, and outage probability for the whole network can be divided into independent hops. The energy consumption and end-to-end delay of the multi-hop network are the summation of the energy consumption and transmission delay inside each hop, while the outage probability is calculated based on the fact that the network will be outage if any one hop is outage.

For the convenience of illustration, a linear uniform multi-hop network [3] is shown in Fig. 1, in which the distance of each hop is  $d/N_h$ , where  $d$  is the distance between S and D. However, the following discussions in this paper, including the analysis on energy consumption, end-to-end delay and outage probability performances are still valid for network topologies other than linear, or for the case of different distances between the hops, as long as the above assumptions are satisfied.

**B. UNDERWATER ENERGY CONSUMPTION MODEL**

Usually, underwater acoustic data transmission can be described by the passive sonar equation. Then the SNR at the receiver can be presented as follows [3],

$$SNR = SL - TL - NL + DI, \tag{1}$$

where  $SL$ ,  $TL$ ,  $NL$  and  $DI$  are, in dB, the source level, transmission loss, noise level and directivity index respectively. When adopting omnidirectional hydrophones, the directivity index is set as 0.

**A. NETWORK TOPOLOGY**

As shown in Fig. 1, we consider a cooperative  $N_h$ -hop UW-ASN consisting of the source node S,  $N_h-1$  relay nodes, and the destination node D, with several cooperative nodes among them. The relay can be expressed as  $R_i$  ( $i = 1, 2, N_h - 1$ ), and the cooperative node is written as  $C_i$  ( $i = 1, 2, N_h$ ).

We have adopted the following assumptions for each hop transmission in the network:

- 1) Nodes are in half-duplex where nodes cannot transmit and receive data at the same time;
- 2) As the focuses are primarily on the ARQ issues, we assume that all the medium access control issues have been resolved. Therefore, the so-called source-relay-destination three nodes in each hop are actually upgraded as  $R_{i-1}-C_i-R_i$  in the multi-hop UW-ASNs scenario. Further, it's assumed that, the transmission of  $R_{i-1}$  can only be received by the two neighboring relay nodes, i.e.,  $R_i$  and  $R_{i-2}$ ; and

For a transmission distance  $d$  in meter and frequency  $f$  in kHz, the transmission loss TL is given by [16]

$$TL = k \cdot 10 \log_{10} (d) + \alpha (f) \cdot d \cdot 10^{-3}, \quad (2)$$

where the first term is the spreading loss with  $k$  represents the the spreading factor, and the second term is the absorption loss with  $\alpha (f)$  represents the absorption coefficient in dB/km. Commonly, the spreading factor  $k$  can be set as 1.5 in practical spreading for underwater acoustic transmission. Following Thorp's formula [17], the absorption coefficient is:

$$\alpha (f) = \frac{0.11f^2}{1+f^2} + \frac{44f^2}{4100+f^2} + 2.75 \times 10^{-4} f^2 + 0.003. \quad (3)$$

The ocean ambient noise is modeled by Gaussian statistics and the Power Spectral Density (PSD). Four different noise sources are usually considered: turbulence, shipping, waves and thermal noise. Their strength can be respectively expressed as (in dB re  $\mu$  Pa per Hz) [3]

$$\begin{aligned} NL_t &= 10 \log N_t (f) = 17 - 30 \log f \\ NL_s &= 10 \log N_s (f) = 40 + 20 (s - 0.5) \\ &\quad + 26 \log f - 60 \log (f + 0.03) \\ NL_w &= 10 \log N_w (f) = 50 + 7.5w^{(1/2)} \\ &\quad + 20 \log f - 40 \log (f + 0.4) \\ NL_{th} &= 10 \log N_{th} (f) = -15 + 20 \log f, \end{aligned} \quad (4)$$

where  $s$  is the shipping activity factor,  $w$  is the wind speed in m/s. Define  $NL_i (f)$  ( $i \in N^- = \{t, s, w, th\}$ ), then the total noise is:

$$N (f) = N_t (f) + N_s (f) + N_w (f) + N_{th} (f). \quad (5)$$

Expressed in dB, that is

$$NL = 10 \log N (f) = 10 \log \sum_{i \in N^-} 10^{NL_i/10}. \quad (6)$$

From (1), obviously, for a given receiver SNR<sub>0</sub> with known  $TL$  and  $NL$ , the energy consumption at the transmitter can be calculated from the source level  $SL$ . And the  $SL$  is given by [16]

$$SL = 10 \log_{10} \frac{I_t}{I_{ref}}, \quad (7)$$

where  $I_t$  is the intensity of the sound emitted by the transmitter, and the reference intensity  $I_{ref}$  in underwater sound [16] is usually the intensity of a plane wave having an root-mean-square pressure equal to 1  $\mu$ Pa, denoted as  $I_{ref} \approx 0.667 \times 10^{-18}$  W/m<sup>2</sup>. That is related to the effective sound pressure, the density of sea water, and the propagation velocity of sound wave  $c$  in sea water. Without loss of generality, we assume a constant speed of  $c = 1500$  m/s.

In the case of cylindrical spreading, the power  $P_t$  required to achieve intensity  $I_t$  at 1 meter from the source in the direction of the receiver is [17]:

$$P_t = 2\pi z I_t, \quad (8)$$

where  $P_t$  is in watt and  $z$  is the water depth in meter.

According to (1), (2), (6), (7) and (8), with the optimal frequency  $f_0$  for a given  $d$ , the power  $P_t$  can be expressed as

$$P_t = 2\pi z_0 I_{ref} 10^{\frac{TL+NL+SNR_0}{10}} |_{f=f_0}, \quad (9)$$

where SNR<sub>0</sub> and  $z_0$  are the corresponding SNR and  $z$  in practical design when operating on the optimal frequency  $f_0$ .

For the commercial hydrophone [18], it consumes about one fifth of the transmitted energy at the receiver for a packet. Then, the energy consumed at the transmitter  $E_t$  and the receiver  $E_r$  can be written as

$$E_t = P_t \times \frac{l}{b} = P_t \times T_l, \quad (10)$$

$$E_r = \frac{1}{5} E_t, \quad (11)$$

where  $l$  is the length of the packet in bits,  $b$  is the bit rate in bps,  $T_l$  is the time cost for transmitting  $l$  bits in second.

### III. THE PROPOSED S-DCC PROTOCOL FOR MULTI-HOP UW-ASNS

#### A. SELECTIVE DYNAMIC CODED COOPERATIVE PROTOCOL

Consider a burst-based transmission for the multi-hop UW-ASNs in the following discussion. Each burst consists of  $N_{bl}$  blocks, and we take the OFDM block as the example for analysis [14]. Over the  $N_{bl}$  blocks, we use erasure-correction channel code for the inter-block encoding, which is the foundation for coded cooperation at relays.

Before illustrating the S-DCC protocol, we first briefly introduce the conventional stop and wait ARQ (S&W ARQ) protocol, the cooperative ARQ (C-ARQ) protocol and the dynamic coded cooperation (DCC) protocol in [13], [15], [19]. They are illustrated in Figs. 2 (a), (b) and (c) respectively, where the  $(i-1)$ -th relay node  $R_{i-1}$  is the transmitter, and the  $i$ -th relay node  $R_i$  is the receiver. In each "R<sub>*i-1*</sub>-C<sub>*i*</sub>-R<sub>*i*</sub>" transmission unit, when adopting the S&W ARQ protocol, the receiver will send a NAK signal to the transmitter for retransmission request if it cannot decode the blocks correctly, while it is to the cooperative node when adopting the C-ARQ protocol. Therefore, the C-ARQ protocol can improve the transmission success rate since the cooperative node is located between the transmitter and receiver. In the meanwhile, it can reduce the end-to-end delay because both NAK signal and retransmission happen in a shorter distance, as shown in Fig. 2 (b). Furthermore, when adopting the DCC protocol, the cooperative node only retransmits part of blocks (say  $N_{li}$  blocks) instead of all the blocks (say  $N_{bl}$  blocks) as shown in Fig. 2 (c) once retransmission occurs. It can further reduce the end-to-end delay because of the shorter retransmission time; meanwhile, the  $N_{li}$  blocks can be added to the front of  $N_{coop}$  blocks for joint decoding and it can improve the performance of decoding [13].

However, in DCC protocol, after sending a NAK signal to the cooperative node  $C_i$ , the receiver  $R_i$  still needs to wait



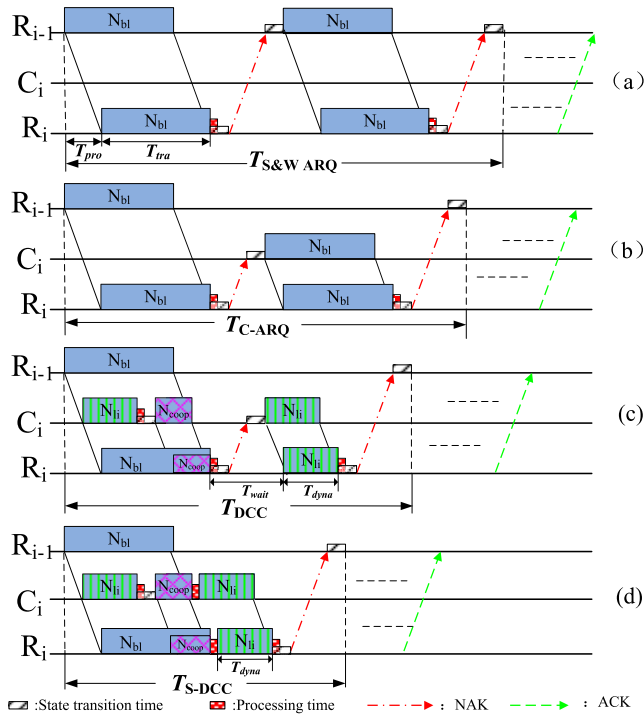


**FIGURE 2. Different cooperation schemes for each hop in multi-hop UW-ASNs: (a) Conventional stop and wait ARQ (S&W ARQ) protocol; (b) Cooperative ARQ (C-ARQ) protocol; (c) Dynamic Coded Cooperation (DCC) protocol; (d) Selective Dynamic Coded Cooperation (S-DCC) protocol.**

for the retransmission from node  $C_i$ . Since both NAK signal and data retransmission still occupy extra time, the receiver is in idle in the  $T_{wait}$  period. To further eliminate this waiting time, we propose that the cooperative node  $C_i$  retransmits the  $N_{li}$  listening blocks immediately after the  $N_{coop}$  cooperation blocks, and then the receiver  $R_i$  can take different actions on these  $N_{li}$  blocks, depending on its instant decoding results. The proposed scheme can shorten the NAK signal's transmission time, and especially it can observably shorten the overall end-to-end delay for the multi-hop UW-ASNs due to the accumulated benefit. As the receiver selectively handles with the redundant  $N_{li}$  blocks, we name it as selective dynamic coded cooperative (S-DCC) protocol.

For the S-DCC protocol, to get a reliable transmission in each hop, it works in the following steps.

1) ACTIVE RETRANSMITTING BASED ON BURST TRANSMISSION: during the listening phase, the cooperative node  $C_i$  try to carry out instantaneous decoding every time receiving one more block from node  $R_{i-1}$ ; immediately after the information bits within one burst are successfully recovered, say  $N_{li}$  blocks, the cooperative node  $C_i$  regenerates the coded transmission blocks, say  $N_{coop} = N_{bl} - N_{li}$  blocks, and switches to cooperative phase and relays the data to node  $R_i$ . After this, the cooperative node  $C_i$  will actively retransmits the first  $N_{li}$  blocks following the  $N_{coop}$  blocks under a given period of time, say  $T_{dyna}$ , as shown in Fig. 2 (d).

2) SELECTIVE RECEIVING BASED ON JOINT DECODING: the receiver node  $R_i$  will firstly carry out joint

decoding by combining the  $N_{bl}$  blocks from node  $R_{i-1}$  with the last  $N_{coop}$  blocks from cooperative node  $C_i$ ; if it is unable to decode correctly, the receiver node  $R_i$  will receive the following retransmitted  $N_{li}$  blocks from cooperative node  $C_i$ , which can be added to the previously available  $N_{bl}$  blocks for joint decoding; if the receiver decodes correctly, it will skip these retransmitted  $N_{li}$  blocks and send ACK signal to the transmitter node  $R_{i-1}$ .

Note that the cooperative node can retransmit  $N_{li}$  blocks several times until reaching the given maximum retransmission time. And the receiver may carry out joint decoding upon the received  $N_{bl}$  blocks,  $N_{coop}$  blocks and all the retransmitted  $N_{li}$  blocks depending on the underwater acoustic channel state. However, as the underwater acoustic modem is working on half-duplex mechanism, the cooperative node can not receive the ACK signal from the receiver during its retransmission of the  $N_{li}$  blocks to the receiver. Hence the retransmit time can not be set too large, which is determined by the underwater acoustic channel states, the length of the  $N_{li}$  blocks, and the distance between the cooperative node and the receiver node. We will adjust this parameter by simulation in the following.

## B. ENERGY CONSUMPTION

The summation of the energy consumption in each hop can be described as

$$E_{total} = \sum_{i=1}^{N_h} E_{hop,i}, \quad (12)$$

where  $E_{hop,i}$  is the energy consumed in the  $i$ -th hop. The energy consumed in transmitting and receiving one block is represented as  $E_{tx}^{block}$  and  $E_{rx}^{block}$  respectively. When operating in the idle mode, the energy consumed is written as  $E_{Idle}$ . Then we can further express the energy consumption as:

$$\begin{aligned} E_{tx}^{block} &= P_t \times T_{block} \\ E_{rx}^{block} &= P_r \times T_{block} \\ E_{Idle} &= P_{Idle} \times T_{Idle}, \end{aligned} \quad (13)$$

where  $P_t$ ,  $P_r$ ,  $P_{Idle}$ ,  $T_{block}$  and  $T_{Idle}$  are the transmission power, reception power, idle mode operating power, block transmission time and idle mode operating time, respectively. Besides, the energy consumption of transmitting and receiving an ACK or NAK signal can be expressed as  $E_{tx}^{ACK/NAK}$  and  $E_{rx}^{ACK/NAK}$  respectively. In this paper, we assume the duration and energy consumption of ACK are equal to those of the NAK because of the same length.

Following Section II A, the analysis of the energy consumption of the whole network can be divided into each independent hop. For the  $i$ -th hop, i.e., the " $R_{i-1}$ - $C_i$ - $R_i$ " unit in the multi-hop UW-ASNs scenario as shown in Fig. 2, the total energy consumption can be calculated as:

$$E_{hop,i} = E_{R_{i-1}} + E_{C_i} + E_{R_i}, \quad (14)$$

where  $E_{R_{i-1}}$ ,  $E_{C_i}$  and  $E_{R_i}$  are the energy consumed at transmitter node  $R_{i-1}$ , the cooperative node  $C_i$  and receiver node

$R_i$ , respectively. In particular, we assume the transmitter node  $R_{i-1}$  transmits a packet comprising  $N_{bl}$  blocks data for  $T_x$  times in total, invoking a total of  $T_x$  cooperation processes in the cooperative node  $C_i$ , until the packet is successfully delivered to the receiver node  $R_i$ ; during each cooperation process, such as the  $T_x$ -th cooperation process, the cooperative node  $C_i$  retransmits  $C_x$  times of the  $N_{li}$  blocks, until the receiver node  $R_i$  successfully decoded all the  $N_{bl}$  blocks. When  $T_x = u$  and  $C_x = v$ , (14) can be written as

$$E_{hop,i} \Big|_{\substack{T_x=u \\ C_x=v}} = E_{R_{i-1},i} \Big|_{\substack{T_x=u \\ C_x=v}} + E_{C_i,i} \Big|_{\substack{T_x=u \\ C_x=v}} + E_{R_i,i} \Big|_{\substack{T_x=u \\ C_x=v}} \quad (15)$$

Furthermore, we define  $\Pr\{T_x = u, C_x = v\}$  to be the probability that for a successful delivery it takes  $T_x = u$  times packet transmissions from the transmitter, and the final delivery coming after  $C_x = v$  times cooperation have been required, with  $u \in \{1, 2, 3, \dots, \infty\}$  and  $v \in \{0, 1, 2, \dots, M_{max}\}$ , where  $M_{max}$  represents the maximum transmission times of the cooperative node  $C_i$ . Let  $E_{hop,i} \in \{E_{S-DCC,i}, E_{C-ARQ,i}, E_{DCC,i}\}$  denote three different protocols, then we have the final expression of energy consumption as:

$$E_{hop,i} = \sum_{u=1}^{\infty} \sum_{v=0}^{M_{max}} E_{hop,i} \Big|_{\substack{T_x=u \\ C_x=v}} \times \Pr\{T_x = u, C_x = v\}, \quad (16)$$

where  $E_{hop,i} \in \{E_{S-DCC,i}, E_{C-ARQ,i}, E_{DCC,i}\}$  and

$$E_{hop,i} \Big|_{\substack{T_x=u \\ C_x=v}} \in \left\{ E_{S-DCC,i} \Big|_{\substack{T_x=u \\ C_x=v}}, E_{C-ARQ,i} \Big|_{\substack{T_x=u \\ C_x=v}}, E_{DCC,i} \Big|_{\substack{T_x=u \\ C_x=v}} \right\},$$

correspondingly.

Now let's derive the energy consumption of S-DCC protocol  $E_{S-DCC,i}$  first. When  $T_x = u$  and  $C_x = v$ , the energy consumption of the transmitter node  $R_{i-1}$  to transmit  $N_{bl}$  blocks can be given by:

$$E_{R_{i-1},i} \Big|_{\substack{T_x=u \\ C_x=v}} = uE_{tx}^{data} + (u-1)E_{rx}^{NAK} + E_{rx}^{ACK} + uE_{Idle}^{R_{i-1}} \\ = u \left( N_{bl}E_{tx}^{block} + E_{rx}^{ACK/NAK} + E_{Idle}^{R_{i-1}} \right) \quad (17)$$

where  $E_{tx}^{data}$  is the energy consumption of transmitting the  $N_{bl}$  blocks data.

Then, the energy consumption at the cooperative node  $C_i$  and receiver node  $R_i$  can be similarly presented as:

$$E_{C_i,i} \Big|_{\substack{T_x=u \\ C_x=v}} = u \left( N_{li}E_{rx}^{block} + N_{coop}E_{tx}^{block} + vN_{li}E_{tx}^{block} + E_{Idle}^{C_i} \right) \quad (18)$$

$$E_{R_i,i} \Big|_{\substack{T_x=u \\ C_x=v}} = u \left( N_{bl}E_{rx}^{block} + vE_{dyna}^{S-DCC} + E_{tx}^{ACK/NAK} + E_{Idle}^{R_i} \right), \quad (19)$$

where

$$E_{dyna}^{S-DCC} = \begin{cases} N_{li}E_{rx}^{block}, & j = 0 \\ 0, & j = 1 \end{cases} \quad (20)$$

When  $j = 0$ , it means that the receiver can not decode correctly after receiving  $N_{coop}$  blocks and thus require the cooperative  $N_{li}$  data blocks for joint decoding.

Since the receiver node  $R_i$  receives the  $N_{bl}$  blocks from the transmitter node  $R_{i-1}$  and  $N_{coop}$  blocks from the cooperative node  $C_i$  at the same time, and the duration time of  $N_{bl}$  blocks is longer than that of  $N_{coop}$  blocks, we can only calculate the duration time of  $N_{bl}$  blocks in (19). That is why the energy consumption of receiving the  $N_{coop}$  blocks do not show up in (19).

Above all, plug (17), (18) and (19) into (15), for the S-DCC protocol in the  $i$ -th hop, we have:

$$E_{S-DCC,i} \Big|_{\substack{T_x=u \\ C_x=v}} = E_{R_{i-1},i} \Big|_{\substack{T_x=u \\ C_x=v}} + E_{C_i,i} \Big|_{\substack{T_x=u \\ C_x=v}} + E_{R_i,i} \Big|_{\substack{T_x=u \\ C_x=v}} \\ = u \left\{ \begin{aligned} &(N_{bl} + N_{coop})E_{tx}^{block} + (N_{li} + N_{bl})E_{rx}^{block} \\ &+ v \left( N_{li}E_{tx}^{block} + E_{dyna}^{S-DCC} \right) + E_{rx}^{ACK/NAK} + E_{tx}^{ACK/NAK} \\ &+ E_{Idle}^{R_{i-1}} + E_{Idle}^{C_i} + E_{Idle}^{R_i} \end{aligned} \right\} \quad (21)$$

Similarly, for the other two cooperative protocols, we have (22) and (23), as shown at the top of the next page, where

$$E_{dyna}^{DCC} = \left( E_{tx}^{block} + E_{rx}^{block} \right) N_{li} + E_{tx}^{ACK/NAK} + E_{rx}^{ACK/NAK} \quad (24)$$

Therefore, with (21), (22) and (23) in hand, we can use (16) to calculate the energy consumption for the three different protocols.

### C. END-TO-END DELAY

Similar to the derivation of energy consumption, we will briefly present the derivation of the end-to-end delay for the three different protocols in the following. The aggregated delay of each hop can be presented as

$$T_{total} = \sum_{i=1}^{N_h} T_{hop,i} \quad (25)$$

Due to the independence between hops, we focus on the delay analysis of one hop. For the  $i$ -th hop, the end-to-end delay comprising the propagation delay and the transmission latency:

$$T_{hop,i} = T_{pro,i} + T_{tra,i} \quad (26)$$

where the propagation delay  $T_{pro,i}$  is related to the retransmission time, the end-to-end distance, the sound velocity in water, and different cooperation protocols. In each hop, let  $T_{pro}$  be equal to the relay-to-relay distance divided by the sound velocity in water for one transmission, i.e.,  $T_{pro} = \frac{d}{N_h \cdot c}$ . For the case of different distances between hops,  $T_{pro}$  and  $d/N_h$  should be modified as  $T_{pro,i}$  and  $d_i$  (the distance in the  $i$ -th hop), respectively. And  $T_{tra,i}$  is the transmission time of a burst packet in each hop. It is related to the block time duration and the number of blocks. Denote  $T_{bl}$  as one

$$E_{C-ARQ,i} \Big|_{\substack{Tx=u \\ Cx=v}} = u \left\{ \begin{aligned} & (E_{tx}^{block} + 2E_{rx}^{block}) N_{bl} + v \left[ \begin{aligned} & (E_{tx}^{block} + E_{rx}^{block}) N_{bl} \\ & + E_{tx}^{ACK/NAK} + E_{rx}^{ACK/NAK} \end{aligned} \right] \\ & + E_{tx}^{ACK/NAK} + E_{rx}^{ACK/NAK} + E_{Idle}^{R_{i-1}} + E_{Idle}^{C_i} + E_{Idle}^{R_i} \end{aligned} \right\} \quad (22)$$

$$E_{DCC,i} \Big|_{\substack{Tx=u \\ Cx=v}} = u \left[ \begin{aligned} & (N_{bl} + N_{coop}) E_{tx}^{block} + (N_{bl} + N_{li}) E_{rx}^{block} \\ & + v E_{tx}^{DCC} + E_{tx}^{ACK/NAK} + E_{rx}^{ACK/NAK} \\ & + E_{Idle}^{R_{i-1}} + E_{Idle}^{C_i} + E_{Idle}^{R_i} \end{aligned} \right] \quad (23)$$

block time-duration, then  $T_{tra} = N_{bl} T_{bl}$  for one transmission. Assume the ACK, NAK signal duration is  $T_{ck}$ . In the following, let  $T_{hop,i} \in \{T_{C-ARQ,i}, T_{DCC,i}, T_{S-DCC,i}\}$  denote the delay corresponding to three different protocols.

Define  $T_{str}$  and  $T_{dec}$  as the state transition delay, the node processing time, respectively. Synchronizing the reception blocks has been illustrated in [13]. Thus, according to Fig.2, let  $T_x = u$  and  $C_x = v$ , for the C-ARQ protocol, DCC protocol and S-DCC protocol, we can derive that

$$T_{C-ARQ,i} \Big|_{\substack{Tx=u \\ Cx=v}} = u \left[ \begin{aligned} & 2T_{pro} + T_{tra} + v (T_{pro} + T_{tra} + T_{ck} + 2T_{str}) \\ & + T_{ck} + 2T_{str} \end{aligned} \right] \quad (27)$$

$$T_{DCC,i} \Big|_{\substack{Tx=u \\ Cx=v}} = u \left[ \begin{aligned} & 2T_{pro} + T_{tra} + v (T_{pro} + T_{dyna} + T_{ck} + 2T_{str}) \\ & + T_{ck} + 2T_{str} \end{aligned} \right] \quad (28)$$

$$T_{S-DCC,i} \Big|_{\substack{Tx=u \\ Cx=v}} = u \left[ \begin{aligned} & 2T_{pro} + T_{tra} + v (T_{dyna} + T_{dec}) \\ & + T_{ck} + 2T_{str} \end{aligned} \right] \quad (29)$$

where  $T_{dyna}$  is the dynamic transmission time for the cooperative node to retransmit the blocks in the DCC or S-DCC protocol, and can be expressed as

$$T_{dyna} = N_{li} T_{bl} \quad (30)$$

Introducing the  $\Pr\{T_x = u, C_x = v\}$ , we have the final expression of end-to-end delay as

$$T_{hop,i} = \sum_{u=1}^{\infty} \sum_{v=0}^{M_{max}} T_{hop,i} \Big|_{\substack{Tx=u \\ Cx=v}} \times \Pr\{T_x = u, C_x = v\} \quad (31)$$

where  $T_{hop,i} \in \{T_{C-ARQ,i}, T_{DCC,i}, T_{S-DCC,i}\}$  and

$$T_{hop,i} \Big|_{\substack{Tx=u \\ Cx=v}} = \left\{ T_{C-ARQ,i} \Big|_{\substack{Tx=u \\ Cx=v}}, T_{DCC,i} \Big|_{\substack{Tx=u \\ Cx=v}}, T_{S-DCC,i} \Big|_{\substack{Tx=u \\ Cx=v}} \right\},$$

correspondingly.

The theoretical calculation of  $\Pr\{T_x = u, C_x = v\}$  is beyond the scope of this paper, hence computer simulations are used instead.

## IV. NUMERICAL RESULTS

### A. SIMULATION SETUP

For the  $N_h$ -hop UW-ASNs network, let  $N_h = 5$ , and the distance in each hop is  $d/N_h = 2$  km. In each burst packet, let the transmission data burst size be  $N_{bl} = 20$  blocks coded over  $I_{bl} = 10$  information blocks, then the information rate is  $r = 0.5$  bit/symbol. The OFDM parameters of the transmitter are the same as those in [20], such as subcarrier number  $K = 1024$ , center frequency  $f_c = 10$  kHz. We use the quasi-static fading underwater acoustic channel model, where the multi-path channels are randomly generated with 50 taps in the baseband [2], [14]. Without loss of generality, in the “ $R_{i-1}$ - $C_i$ - $R_i$ ” unit, we set the transmission times of  $R_{i-1}$  is only once, and the maximum number of transmissions of the cooperative node  $C_i$  is also one during the simulation, i.e.,  $\{u, M_{max}\} = \{1, 1\}$ . This is the general parameter setting except during the study of impact of different  $M_{max}$  values. In addition, to evaluate the energy consumption and end-to-end delay, we use Monte Carlo method to obtain the results according to (12) and (25).

Instead of a practical code, we assume the erasure-correction codes are capacity-achieving codes thus the mutual information (MI) can be adopted to calculate the outage probability of the transmission, which can indicate whether a packet can be decoded correctly at the receiver. For the node-to-node transmission with  $K$  OFDM sub-carriers, an outage occurs if the total MI at the destination is lower than the information rate  $r$ , which can be expressed as:

$$\begin{aligned} P^{out} &= \Pr\{MI < r\} \\ &= \Pr\left\{ \frac{1}{K} \sum_{k=-K/2}^{K/2-1} \log_2 \left( 1 + |H[k]|^2 \cdot E_s/N_0 \right) < r \right\}, \end{aligned} \quad (32)$$

where  $H[k]$  is the channel complex equivalent factor at the  $k$ -th subcarrier, and  $E_s/N_0$  is the SNR at the receiver node.

Specifically, for the S-DCC protocol, in the  $i$ -th hop, the outage probability can be calculated in (33), as shown at the bottom of the next page where  $H_{sd}$  denotes the channel frequency response between the source and the destination,  $H_{rd}$  denotes the channel frequency response between the cooperative node and the destination, and  $j = 0$  or 1. When  $j = 0$ , it regresses to DCC protocol; when  $j = 1$ , it means that

the receiver can not decode correctly after receiving  $N_{\text{coop}}$  blocks and thus requires the cooperative  $N_{\text{li}}$  data blocks for joint decoding.

In the multi-hop network where the information is transmitted hop by hop and the signal transmission in one hop will not affect the other hops, each hop will have independent probability of outage and the network outage will happen if any hop is outage. Then the outage probability of the whole  $N_h$ -hop system is

$$P_{S-DCC}^{\text{out}} = 1 - \prod_{i=1}^{N_h} (1 - P_{S-DCC,i}^{\text{out}}) \quad (34)$$

**B. SIMULATION RESULTS**

1) IMPACT OF DIFFERENT PROTOCOLS

Fig. 3 (a) demonstrates the overall outage probability of S-DCC protocol and other protocols. We can see that the proposed S-DCC protocol is slightly better than C-ARQ protocol and overlaps with DCC protocol, and all of them outperform the S&W ARQ protocol. As shown in Fig. 3(b), the proposed S-DCC protocol has the minimum end-to-end delay among these protocols. Especially, for  $P^{\text{out}} \leq 10^{-2}$  ( $P/\sigma_w^2 = 47 - 48\text{dB}$ , where  $P/\sigma_w^2 := SL - NL$  is the transmission SNR in dB), the performance of end-to-end delay of S-DCC is better than that of DCC because of the new retransmission mechanism for S-DCC. Specifically, the S-DCC protocol can eliminate the feedback signal from the  $R_i$  node to  $C_i$  node and hence reduces the overall end-to-end delay in retransmission. However, performances of S-DCC and DCC become close at high transmission SNR region, and this is because no more retransmissions are needed for both of them as the transmission SNR increases. Therefore, the proposed S-DCC protocol can achieve good outage performance while reducing the end-to-end delay, relative to existing protocols. Since (A) the outage performance of S&W ARQ protocol is much worse than the other three cooperative protocols, which is extremely detrimental to the multi-hop UW-ASNs scenario. And all the cooperative protocols should have the same energy consumption and time delay happened in the cooperative node selection stage; (B) in a relative static network (as required by DCC, because it needs the exact distance information between the 3 nodes), the energy consumption and time delay happened in the cooperative node selection stage should be insignificant compared with the data transmission, we will skip S&W ARQ and will not include the energy consumption and time delay happened in the cooperative node selection stage. Instead, we focus on

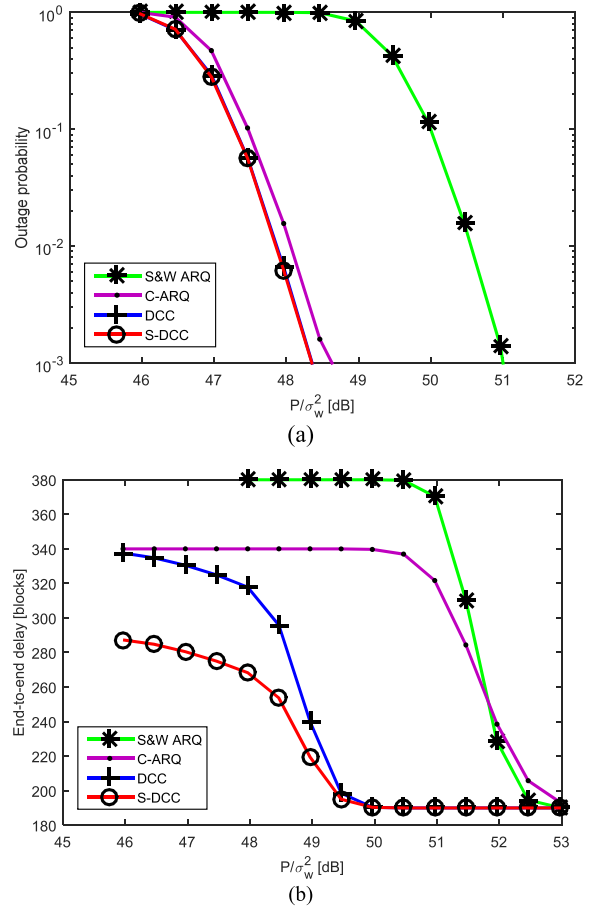


**FIGURE 3. Performance comparison of several network schemes: (a) Overall outage probability; (b) End-to-end delay.**

the comparison of the three cooperative protocols in the data transmission in the following discussions.

To clearly understand energy consumption of the three cooperative protocols, Fig. 4 (a) shows the energy consumption results. It can be found that in the low transmission SNR region (46-48 dB), the energy consumption of S-DCC is slightly lower than the other two protocols, but with the increase of transmission SNR, the energy consumption of S-DCC increases more than DCC. This is because that the receiver only needs one transmission to successfully decode the information without the cooperative node's retransmission at high SNR region. Hence for the S-DCC, the receiver does not use the extra  $N_{\text{li}}$  blocks transmitted by cooperative node, causing additional energy consumption.

$$P_{S-DCC,i}^{\text{out}} = \Pr \{MI < r\} = \Pr \left\{ \frac{1}{K} \sum_{k=-K/2}^{k=K/2-1} \left[ N_{\text{bl}} \log_2 (1 + |H_{sd}[k]|^2 \cdot E_s/N_0) + N_{\text{coop}} \log_2 (1 + |H_{sd}[k] + H_{rd}[k]|^2 \cdot E_s/N_0) \right] < rN_{\text{bl}} \right\}, \quad (33)$$



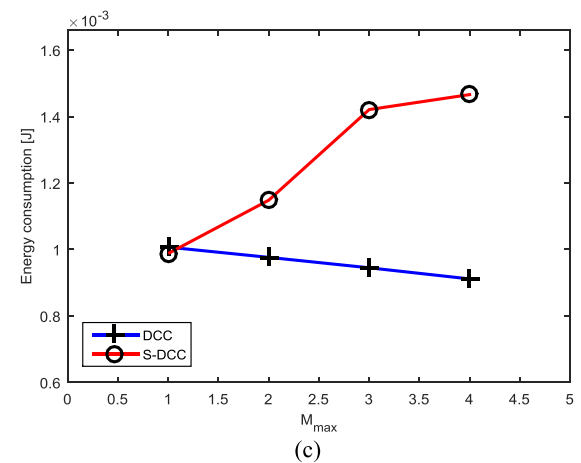
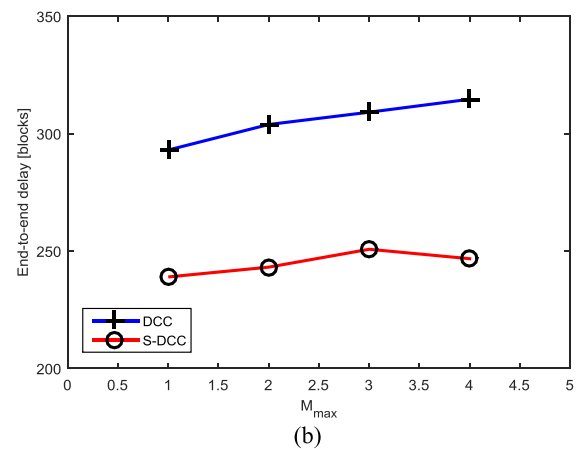
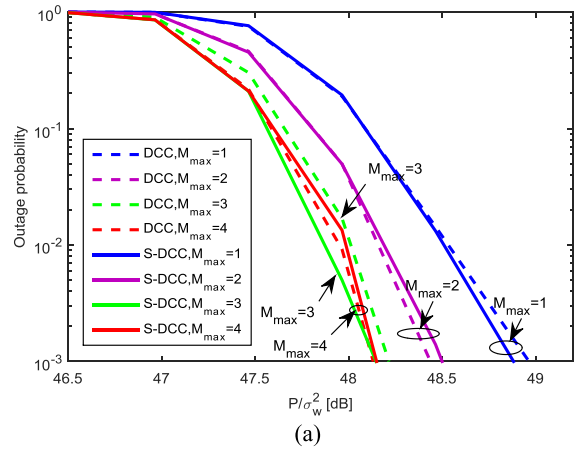
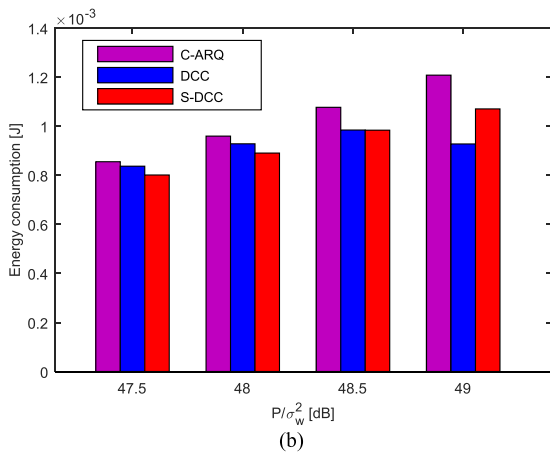
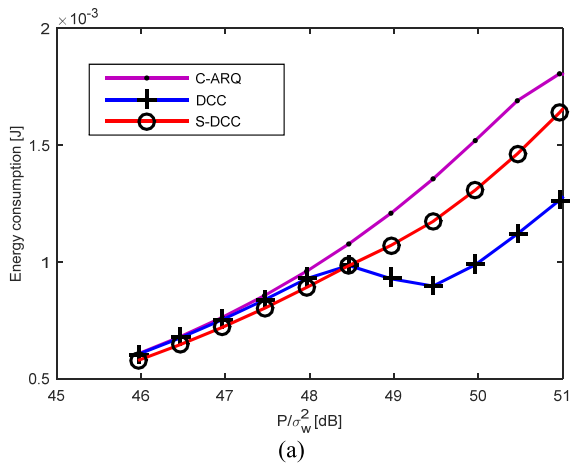


**FIGURE 4. Energy consumptions of several cooperative schemes: (a) Energy consumption; (b) Energy consumption comparison.**

Set the target outage probability of the three cooperative protocols to be  $P^{out} \leq 10^{-2}$ , the corresponding transmission SNR is about 48 dB according to Fig. 3 (a). Fig. 4 (b) shows the comparison of energy consumptions at the transmission SNR around 48 dB. When meeting the outage probability demand, the energy consumption of S-DCC is more economical than the other two schemes at low transmission SNR region.

2) IMPACT OF COOPERATIVE TRANSMISSION TIMES

In (16) and (31), let  $M_{max} \in \{1, 2, 3, 4\}$ ,  $u = 1$ , then the maximum number of cooperative node transmission times is between 1 and 4. To analyze the impact of maximum number of retransmissions, we should ensure that the link between the transmitter and the cooperative node cannot be interrupted. Therefore the cooperative node is closer to the transmitter than to the receiver in each hop. As shown in Fig. 5(a), with the maximum number of retransmissions increasing, the possibility of the receiver decodes correctly increases. Specifically, the cases of  $M_{max} = 2$  and  $M_{max} = 3$  have about 0.5 dB and 0.7 dB gain, respectively, compared with  $M_{max} = 1$ . The overall outage probability of  $M_{max} = 3$  and  $M_{max} = 4$  is similar. Thus, the outage probability will

**FIGURE 5. The impact of the maximum number of retransmissions on system performance: (a) Overall outage probability; (b) End-to-end delay; (c) Energy consumption.**

not increase infinitely with the maximum number of retransmissions increasing. In addition, both S-DCC and DCC have similar overall outage probability under the same setting of maximum number of retransmissions.

Set the target outage probability to be  $P^{out} \leq 10^{-2}$ , the end-to-end delay and the energy consumption of these two schemes are shown in Fig. 5 (b) and Fig. 5 (c). From Fig. 5 (b), we can see that with the number of retransmissions increasing, the end-to-end delay of DCC or S-DCC increases

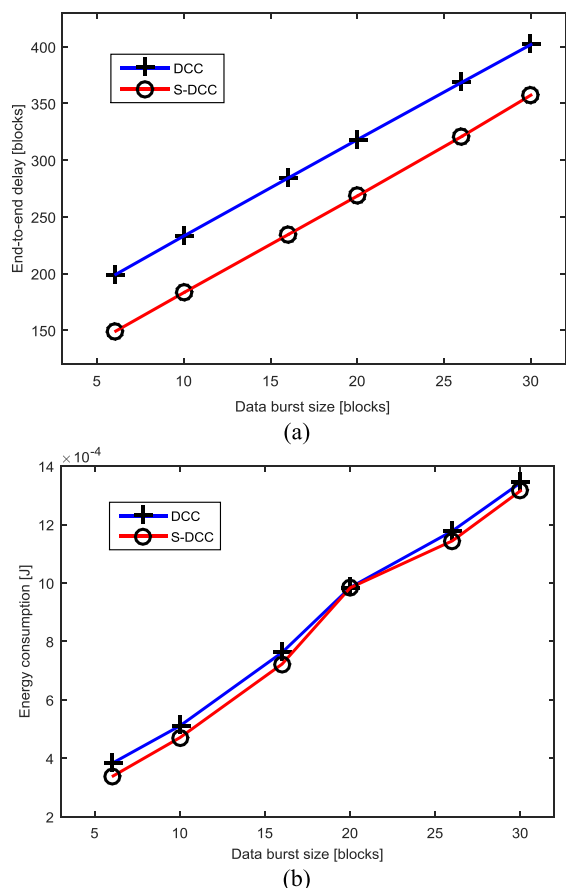


FIGURE 6. The impact of data burst size on system performance: (a) End-to-end delay; (b) Energy consumption.

slightly, and the end-to-end delay of S-DCC is always less than that of DCC. From Fig. 5 (c), the energy consumption of S-DCC increases with the number of retransmissions, while the case for DCC is the opposite. When  $M_{max} = 1$ , the energy consumption of S-DCC is slightly smaller than the DCC, but when  $M_{max} = 2$ , the energy of S-DCC is consumed by more than 10% compared with DCC. This is because at high transmission SNR region, DCC only requests retransmission from the cooperative node as needed, while S-DCC may retransmit unnecessary cooperative blocks without considering the receiver’s decoding results and result in the energy waste. Therefore, at the high transmission SNR region,  $M_{max} = 1$  is usually enough for S-DCC protocol.

### 3) IMPACT OF DATA BURST SIZE

Next, we investigate the impact of the data burst size in unit of block on the end-to-end delay and energy consumption for DCC and S-DCC, where the information rate is fixed at 0.5 bit/symbol. The results with target outage probability performance are shown in Fig. 6. We can see that S-DCC still outperforms DCC for any size setting of data block. This is because in S-DCC, limited direct retransmission of the cooperative blocks eliminates the waiting time of the receiver, and less transmission of feedback signal reduces the energy consumption.

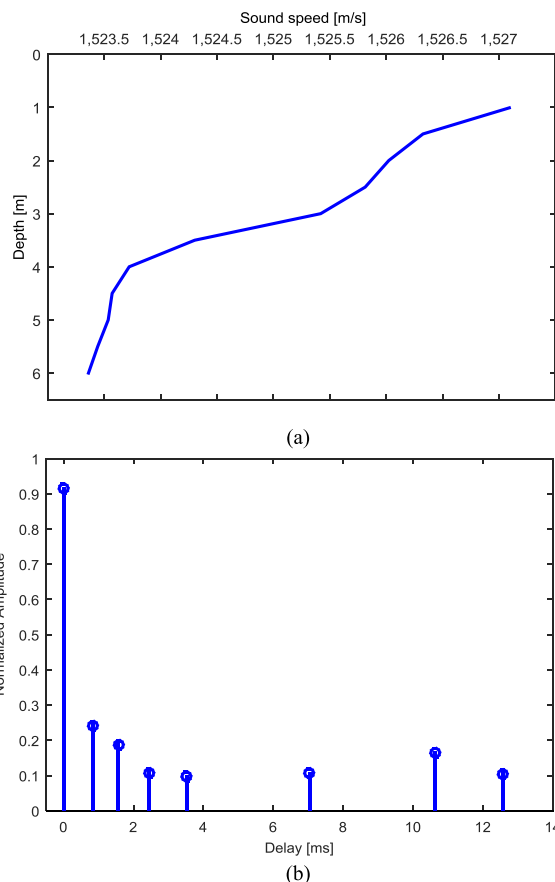


FIGURE 7. Sea test data of underwater acoustic channel for the Xiamen Wuyuan Bay: (a) The sound speed profile; (b) Channel impulse response.

## V. EXPERIMENTAL RESULTS

To further test the performance of S-DCC, the test data from Xiamen Wuyuan bay on May 8, 2014, which lies in the northern part of Xiamen, Fujian, China, are used to set up the underwater acoustic channel model. The depth of the transmitter and the receiver is 3 m and 4 m, respectively. The distance between them is 903 m. The detection signal is the LFM signal, whose duration is 24 ms and frequency range is 20-22 kHz. The sampling frequency is 80 kHz, and there is a 12 ms guard interval after detection signal. Fig. 7 (a) shows the sound speed profile of Xiamen Wuyuan Bay, Fig. 7 (b) presents the channel impulse response of Wuyuan Bay underwater acoustic channel, which have 8 multi-paths and the maximum delay is approximately 12.5 ms. The results are tested in level 3 sea state.

Table 2 shows the performance comparison of these three protocols for Wuyuan Bay sea test channel. As expected, the S-DCC outperforms both C-ARQ and DCC protocols at lower transmission SNR region (the cases of 39.96 dB and 40.96 dB). As the transmission SNR increases (the cases of 41.96 dB and 42.96 dB), once the decoding on the receiver does not need the cooperative node’s retransmission anymore, S-DCC does not have the advantage in end-to-end delay, and its energy consumption is increasing rapidly. This is consistent with the previous analysis.

**TABLE 2. Results based on sea test data channel.**

$P/\sigma_w^2$	$P^{out}$	$T_{total}^a$	$E_{total}^a$
39.96 dB	C-ARQ	1.0000	NA
	DCC	0.2840	253.5754
	S-DCC	0.2960	223.3068
40.96 dB	C-ARQ	1.0000	NA
	DCC	0.0600	230.3191
	S-DCC	0.0360	203.7095
41.96 dB	C-ARQ	0.9760	280.0000
	DCC	0.0240	182.6598
	S-DCC	0.0002	170.3920
42.96 dB	C-ARQ	0.7920	278.5000
	DCC	0.0002	154.1680
	S-DCC	0.0002	153.3600

<sup>a</sup> End-to-end delay units are data blocks; energy consumption units are J; NA means we didn't get the test data due to the poor link, i.e., the outage probability is 100%.

## VI. CONCLUSION

In this paper, we investigate the improved dynamic coded cooperative protocol named as S-DCC for multi-hop UW-ASNs in terms of end-to-end delay and energy consumption. Compared with S&W ARQ, C-ARQ and DCC protocols, numerical results show that the proposed S-DCC protocol can achieve decent outage performance while reducing end-to-end delay by selective cooperation, without extra energy consumption. Particularly, the S-DCC is a feasible cooperative strategy for low transmission SNR cases.

## ACKNOWLEDGMENT

The authors would like to thank Mr. Shenqin Huang and Mr. Jianming Wu from Xiamen University for their contributions to the discussion of this research. Key Laboratory of Underwater Acoustic Communication and Marine Information Technology and Shenzhen Research Institute of Xiamen University contributed equally to this work.

## REFERENCES

- [1] S. M. Ghoreyshi, A. Shahrabi, T. Boutaleb, and M. Khalily, "Mobile data gathering with hop-constrained clustering in underwater sensor networks," *IEEE Access*, vol. 7, pp. 21118–21132, 2019.
- [2] S. Jiang, "On reliable data transfer in underwater acoustic networks: A survey from networking perspective," *IEEE Commun. Surveys Tuts.*, vol. 20, no. 2, pp. 1036–1055, 2nd Quart. 2018.
- [3] W. Zhang, M. Stojanovic, and U. Mitra, "Analysis of a linear multi-hop underwater acoustic network," *IEEE J. Ocean. Eng.*, vol. 35, no. 4, pp. 961–970, Oct. 2010.
- [4] M. Stojanovic, "On the relationship between capacity and distance in an underwater acoustic communication channel," *ACM SIGMOBILE Mobile Comput. Commun. Rev.*, vol. 11, no. 4, pp. 34–43, Oct. 2007.
- [5] M. Zorzi, P. Casari, N. Baldo, and A. F. Harris, "Energy-efficient routing schemes for underwater acoustic networks," *IEEE J. Sel. Areas Commun.*, vol. 26, no. 9, pp. 1754–1766, Dec. 2008.
- [6] M. Felemban and E. Felemban, "Energy-delay tradeoffs for underwater acoustic sensor networks," in *Proc. 1st Int. Black Sea Conf. Commun. Netw. (BlackSeaCom)*, Jul. 2013, pp. 45–49.
- [7] S. Al-Dharrab, M. Uysal, and T. M. Duman, "Cooperative underwater acoustic communications," *IEEE Commun. Mag.*, vol. 51, no. 7, pp. 146–153, Jul. 2013.

- [8] G. Al-Habian, A. Ghayeb, M. Hasna, and A. Abu-Dayya, "Threshold-based relaying in coded cooperative networks," *IEEE Trans. Veh. Technol.*, vol. 60, no. 1, pp. 123–135, Jan. 2011.
- [9] Q. Li, S. Ting, and C. K. Ho, "A joint network and channel coding strategy for wireless decode-and-forward relay networks," *IEEE Trans. Commun.*, vol. 59, no. 1, pp. 181–193, Jan. 2011.
- [10] J. Castura and Y. Mao, "Rateless coding for wireless relay channels," *IEEE Trans. Wireless Commun.*, vol. 6, no. 5, pp. 1638–1642, May 2007.
- [11] K. Kumar and G. Caire, "Coding and decoding for the dynamic decode and forward relay protocol," *IEEE Trans. Inf. Theory*, vol. 55, no. 7, pp. 3186–3205, Jul. 2009.
- [12] K. Ishibashi, K. Ishii, and H. Ochiai, "Dynamic coded cooperation using multiple turbo codes in wireless relay networks," *IEEE J. Sel. Topics Signal Process.*, vol. 5, no. 1, pp. 197–207, Feb. 2011.
- [13] Y. Chen, Z.-H. Wang, L. Wan, H. Zhou, S. Zhou, and X. Xu, "OFDM-modulated dynamic coded cooperation in underwater acoustic channels," *IEEE J. Ocean. Eng.*, vol. 40, no. 1, pp. 159–168, Jan. 2015.
- [14] Y. Chen, X. Xu, S. Zhou, H. Su, and L. Zhang, "Dynamic coded cooperative ARQ for multi-hop underwater acoustic networks," in *Proc. IEEE OCEANS TAIPEI*, Apr. 2014, pp. 1–5.
- [15] A. Ghosh, J.-W. Lee, and H.-S. Cho, "Throughput and energy efficiency of a cooperative hybrid ARQ protocol for underwater acoustic sensor networks," *Sensors*, vol. 13, no. 11, pp. 15385–15408, Nov. 2013.
- [16] R. J. Urick, *Principles of Underwater Sound*. Los Altos, CA, USA: Peninsula Pub, 1983.
- [17] L. M. Brekhovskikh and Y. P. Lysanov, *Fundamentals of Ocean Acoustics*. New York, NY, USA: Springer, 1982.
- [18] (2007). *LINKQUEST INC. Underwater Acoustic Modem*. [Online]. Available: <http://www.linkquest.com>
- [19] J.-W. Lee and H.-S. Cho, "A cooperative ARQ scheme for multi-hop underwater acoustic sensor networks," in *Proc. IEEE Symp. Underwater Technol. Workshop Sci. Submarine Cables Rel. Technol. (SSC)*, Tokyo, Japan, Apr. 2011, pp. 1–4.
- [20] H. Yan *et al.*, "DSP based receiver implementation for OFDM acoustic modems," *Phys. Commun.*, vol. 5, no. 1, pp. 22–32, Mar. 2012.



**YOUGAN CHEN** (S'12–M'13) received the B.S. degree in communication engineering from Northwestern Polytechnical University (NPU), Xi'an, China, in 2007, and the Ph.D. degree in communication engineering from Xiamen University (XMU), Xiamen, China, in 2012.

He visited the Department of Electrical and Computer Engineering, University of Connecticut (UConn), Storrs, CT, USA, from 2010 to 2012. He has been an Assistant Professor with the Department of Applied Ocean Physics and Engineering, XMU, since 2013. His research interests include communications and signal processing, currently focusing on channel coding and cooperative communications for underwater acoustic channels.

Dr. Chen has served as the Technical Reviewer for many journals and conferences, such as the IEEE JOURNAL OF OCEANIC ENGINEERING, the IEEE TRANSACTIONS ON COMMUNICATIONS, the IEEE ACCESS, *Sensors*, *IET Communications*, and ACM WUWNet Conference. He has been appointed to a 3-year term as Associate Editor in IEEE Access effective May 2019. He served as a Secretary for the IEEE ICSPCC 2017. He received Technological Invention Award of Fujian Province, China, in 2017.



**XIAOTING JIN** received the B.S. degree in marine technology and the M.S. degree in marine physics from Xiamen University (XMU), Xiamen, China, in 2014 and 2017, respectively. She was with XMU, and is currently with the Fujian Provincial Department of Ocean and Fisheries. Her research interests include channel coding, cooperative communications for underwater acoustic channels, and wireless communication and navigation for fishing vessel.



**LEI WAN** (M'18) received the B.S. degree in electronic information engineering from Tianjin University (TJU), Tianjin, China, in 2006, the M.S. degree in signal and information processing from the Beijing University of Posts and Telecommunications (BUPT), Beijing, China, in 2009, and the Ph.D. degree in electrical engineering from University of Connecticut (UConn), Storrs, CT, USA, in 2014.

He is currently an Associate Professor with the College of Underwater Acoustic Engineering, Harbin Engineering University (HEU), Harbin, China. His research interests include the algorithm design, system development, and performance analysis for high speed underwater acoustic communication systems.

Dr. Wan has served as the Technical Reviewer for many journals and conferences. He received the IEEE Communications Society's Exemplary Reviewer Award for the IEEE COMMUNICATIONS LETTERS, in 2013.



**XIAOKANG ZHANG** received the B.S. and Ph.D. degrees in marine physics from Xiamen University (XMU), Xiamen, China, in 2005 and 2010, respectively. From 2010 to 2012, he was a Postdoctoral Research Associate with the Center of Environmental Science and Engineering, XMU. He has been a Senior Engineer with the Department of Applied Marine Physics and Engineering, XMU, since 2012. His research interest includes underwater acoustic communications.



**XIAOMEI XU** received the B.S., M.S., and Ph.D. degrees in marine physics from Xiamen University (XMU), Xiamen, China, in 1982, 1988, and 2002, respectively.

She was a Visiting Scholar with the Department of Electrical and Computer Engineering, Oregon State University, Corvallis, OR, USA, from 1994 to 1995. She visited the Department of Electrical and Computer Engineering, University of Connecticut (UConn), Storrs, CT, USA, as a Senior Visiting Scholar, in 2012. She is currently a Full Professor with the Department of Applied Marine Physics and Engineering, XMU. Her research interests include marine acoustics, underwater acoustic telemetry and remote control, underwater acoustic communication, and signal processing.

...